Available online at www.derpharmachemica.com

ISSN 0975-413X
CODEN (USA): PCHHAX

Der Pharma Chemica, 2016, 8(15):213-226
(http://derpharmachemica.com/archive.html)

A note on the inhibition of steroid 11β-hydroxylase, aldosterone synthase and aromatase by a series of coumarin derivatives

Juan S. Gómez-Jeria[1]* and Gaston A. Kpotin[2]

[1]*Quantum Pharmacology Unit, Department of Chemistry, Faculty of Sciences, University of Chile. Las Palmeras 3425, Santiago 7800003, Chile*
[2]*Laboratory of Theoretical Chemistry and Molecular Spectroscopy, Faculty of Sciences and Technique, University of Abomey-Calavi, 03 BP 3409 Cotonou-Benin*

ABSTRACT

The relationships between the inhibition of steroid 11β-hydroxylase, aldosterone synthase and aromatase enzymes and the electronic structure of a group of coumarin derivatives was analyzed. We obtained statistically significant results for the inhibition of the three enzymes. Some specific molecule-enzyme interactions are suggested. The corresponding pharmacophores were built. Finally, some suggestions that could improve the inhibitory capacity are proposed.

Keywords: Aromatase, coumarin, aldosterone synthase, steroid 11β-hydroxylase, QSAR, DFT, KPG method.

INTRODUCTION

Recently, a paper reporting experimental results of the inhibition of steroid 11β-hydroxylase (also called CYP11B1), aldosterone synthase (also called CYP11B2) and aromatase (also called CYP19) by some coumarin derivatives has interested us to carry out another testing about the validity of the Klopman-Peradejordi-Gómez (KPG) method [1]. These three enzymes are extremely important in human steroidogenesis (Fig. 1) [2-4]. CYP11B1 transforms 11-deoxycortisol into cortisol and 11-deoxycorticosterone to corticosterone. Mutations in the CYP11B1 gene produce steroid 11β-hydroxylase deficiency [5]. CYP11B2 is the only enzyme capable of synthesizing aldosterone in humans and plays a significant role in electrolyte balance and blood pressure. Mutations in the CYP11B2 gene result in aldosterone synthase deficiency, which can cause hyperkalemia, hyponatremia and hypovolemic shock in infancy. The inhibition of CYP11B2 is currently being investigated as a medical treatment for hypertension, heart failure and renal disorders. CYP19 transforms androstenedione to estrone and testosterone to estradiol. Drugs that inhibit the CYP19-mediated synthesis of estrogens in peripheral tissues including the breast are widely used in the treatment of breast cancer. Several studies indicate that overexpression of CYP19 and excessive estrogen production play a role in Leydig cell tumorigenesis. See also [6-14]. Much experimental and theoretical work has been carried out searching for inhibitors of these enzymes [1, 15-35]. Given the interest of this subject, here we present the results of a study analyzing the relationships between the electronic structure of the aforementioned coumarin derivatives and their inhibitory capacity against steroid 11β-hydroxylase, aldosterone synthase and aromatase.

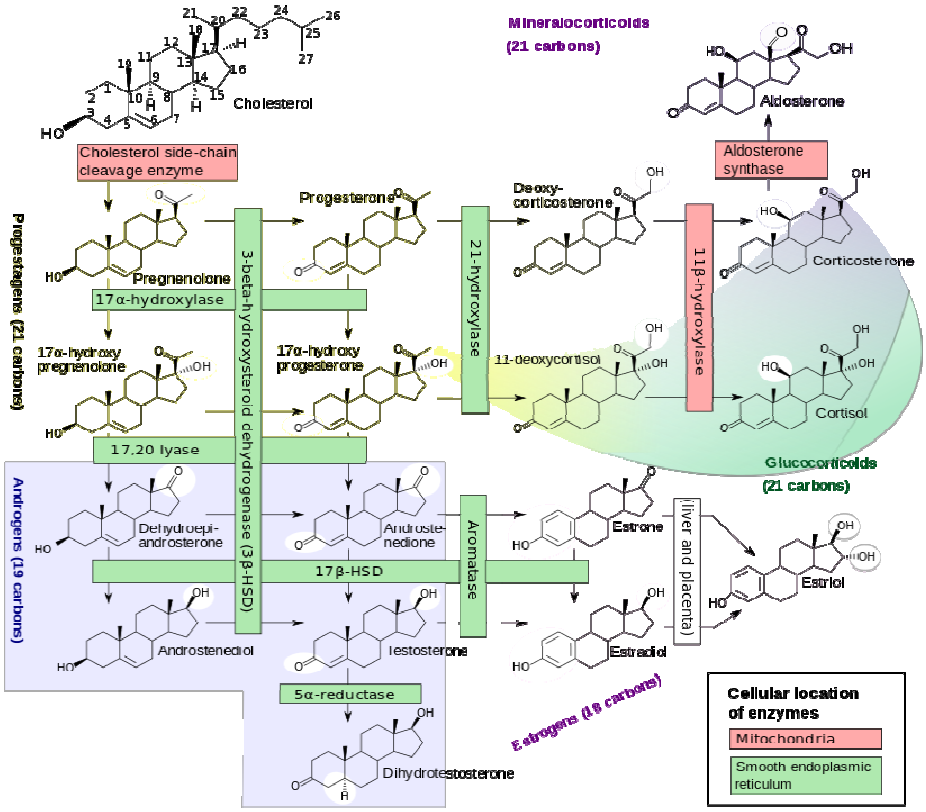

Figure 1. Human steroidogenesis, with the major classes of steroid hormones, individual steroids and enzymatic pathways. Changes in molecular structure from a precursor are highlighted in white. Taken from [36]

Methods, models and calculations.

For this study we employed the Klopman-Peradejordi-Gómez (KPG) formal QSAR method. As this method has been amply discussed in earlier papers, we shall discuss here only the results [37-44]. From the conceptual point of view the work presented here is another test of the hypothesis stating that the KPG model can give an account of the molecule-site equilibrium constants and also provides a formal quantitative relationship between molecular structure and any biological activity. Up today the KPG model shows no failures in its applications [45-55] (and references therein). The selected molecules are a series of coumarin derivatives with inhibitory activity against 11β-hydroxylase (CYP11B1), aldosterone synthase (CYP11B2) and aromatase (CYP19). Molecules and their inhibitory activities are shown in Figure 1 and Table 1 [1].

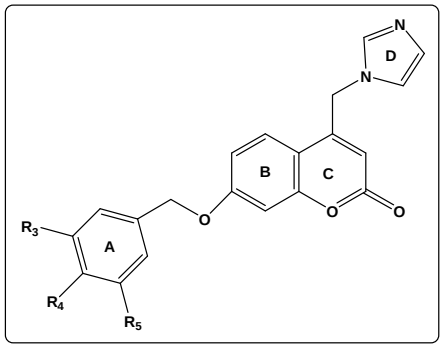

Figure 1. General formulas of coumarin derivatives

Table 1. Coumarin derivatives and inhibitory activities

Mol.	R_3	R_4	R_5	$\log(IC_{50})$ CP11B1	$\log(IC_{50})$ CP11B2	$\log(IC_{50})$ CYP19
1	H	H	H	1.86	2.46	2.18
2	Me	H	H	1.65	2.40	2.06
3	F	H	H	1.60	2.30	2.05
4	Cl	H	H	1.49	2.00	2.11
5	CF_3	H	H	1.30	2.18	2.37
6	OCF_3	H	H	0.70	2.10	2.32
7	NO_2	H	H	1.30	2.00	2.15
8	OMe	H	H	1.68	2.10	2.74
9	H	Cl	H	2.00	2.30	2.25
10	H	OCF_3	H	1.40	2.40	2.68
11	H	NO_2	H	2.05	1.93	2.59
12	H	OMe	H	1.90	2.09	2.1
13	H	$O(CH_2)_2Me$	H	1.80	1.89	2.68
14	H	$OCH(CH_3)_2$	H	1.68	1.91	2.77
15	F	H	F	1.65	2.30	2.23
16	F	F	H	1.70	2.00	2.22
17	OMe	OMe	H	1.76	1.91	2.65
18	OMe	OMe	OMe	1.70	2.17	2.54

The electronic structure of the molecules was calculated with the Density Functional Theory at the B3LYP/6-31g(d,p) level with full geometry optimization. The Gaussian 03 program was used [56]. The numerical values of the local atomic reactivity indices were calculated with the D-Cent-QSAR software [57]. The negative electron populations produced by Mulliken Population Analysis were fixed as usual [58]. The orientational parameters were taken from Tables [59, 60]. Considering that the resolution of the system of linear equations is not possible because we have not enough molecules, we used Linear Multiple Regression Analysis (LMRA) to determine the best solution. For each case, a matrix having the dependent variable (the inhibitory activity of each case) and the local atomic reactivity indices of all atoms of a common skeleton as independent variables was created. To this matrix, the orientational parameters of the R_3, R_4 and R_5 were added. The Statistica software was employed for LMRA [61]. The *common skeleton (CS) approximation* holds that there is a group of atoms, shared by all the molecules analyzed, that accounts for most part of the biological activity. The influence of the substituents consists in altering directly the electronic structure of the CS and inducing the accurate placement of the drug at the action site through the orientational parameters. It is hypothesized that diverse parts or this CS accounts for almost all the interactions leading to the expression of a particular biological activity. The common skeleton is displayed in Fig. 2.

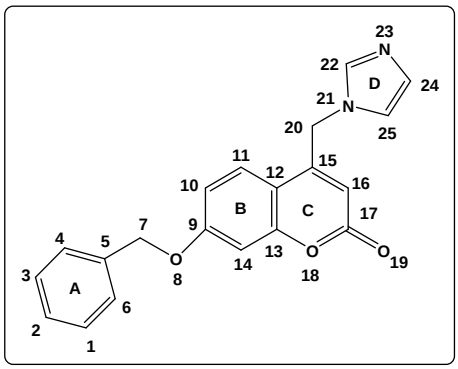

Figure 2. Common skeleton of coumarin derivatives

RESULTS

Results for the inhibition of CYP11B1.

The best equation obtained was:

$$\log(IC_{50})=1.89-0.001\varphi_{R3}-0.59F_1(HOMO-2)^*+3.69F_{22}(LUMO+2)^*+2.01S^E_{18}(HOMO)^* \quad (1)$$

with n=17, R=0.98, R^2=0.96, adj-R^2=0.95, F(4,12)=77.97 (p<0.000001) and SD=0.07. No outliers were detected and no residuals fall outside the ±2σ limits. Here, φ_{R3} is the orientational parameter of the R_3 substituent, F_1(HOMO-2)* is the Fukui index of the third highest occupied MO localized on atom 1, F_{22}(LUMO+2)* is the Fukui index of the third lowest vacant MO localized on atom 22 and S_{18}^E(HOMO)* is the electrophilic superdelocalizability of the highest occupied MO localized on atom 18. Tables 2 and 3 show the beta coefficients, the results of the t-test for significance of coefficients and the matrix of squared correlation coefficients for the variables of Eq. 1. There are no significant internal correlations between independent variables (Table 3). Figure 3 displays the plot of observed *vs*. calculated log(IC_{50}).

Table 2. Beta coefficients and t-test for significance of coefficients in Eq. 1

Variable	Beta	t(12)	p-level
φ_{R3}	-0.83	-13.25	<0.0000001
F_1(HOMO-2)*	-0.23	-3.90	<0.002
F_{22}(LUMO+2)*	0.35	5.28	<0.0002
S_{18}^E(HOMO)*	0.24	3.55	<0.004

Table 3. Matrix of squared correlation coefficients for the variables in Eq. 1

	φ_{R3}	F_1(HOMO-2)*	F_{22}(LUMO+2)*	S_{18}^E(HOMO)*
φ_{R3}	1.00			
F_1(HOMO-2)*	0.05	1.00		
F_{22}(LUMO+2)*	0.00	0.03	1.00	
S_{18}^E(HOMO)*	0.10	0.00	0.21	1.00

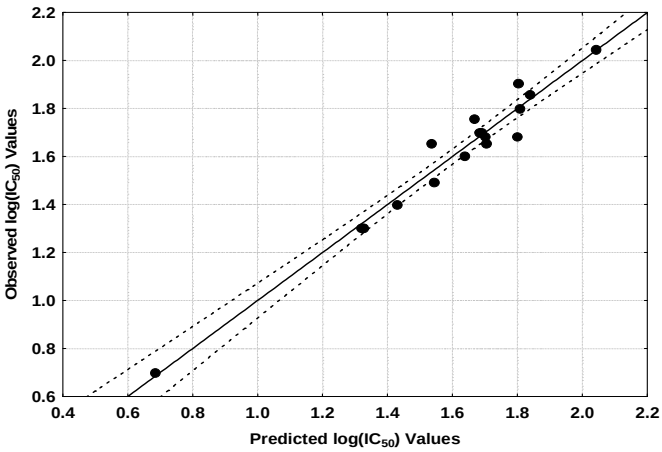

Figure 3. Plot of predicted *vs*. observed log(IC_{50}) values (Eq. 1). Dashed lines denote the 95% confidence interval

The associated statistical parameters of Eq. 1 indicate that this equation is statistically significant and that the variation of the numerical values of a group of four local atomic reactivity indices of atoms of the common skeleton explains about 95% of the variation of log(IC_{50}) in this group of coumarin derivatives. Figure 3, spanning about 1.4 orders of magnitude, shows that there is a good correlation of observed *versus* calculated values.

Results for the inhibition of CYP11B2.
The best equation obtained was:

$$\log(IC_{50})=2.31-0.01S_{10}^{N}(LUMO+2)^*-7.41F_{15}(HOMO-1)^*-0.20S_{20}^{N}(LUMO+2)^* \quad (2)$$

with n=16, R=0.94, R^2=0.87, adj-R^2=0.86, F(3,12)=31.21 (p<0.00001) and SD=0.07. No outliers were detected and no residuals fall outside the ±2σ limits. Here, S_{10}^N(LUMO+2)* is the nucleophilic superdelocalizability of the third

lowest MO localized on atom 10, F_{15}(HOMO-1)* is the Fukui index of the second highest occupied MO localized on atom 15 and S_{20}^{N}(LUMO+2)* is the nucleophilic superdelocalizability of the third lowest vacant MO localized on atom 20. Tables 4 and 5 show the beta coefficients, the results of the t-test for significance of coefficients and the matrix of squared correlation coefficients for the variables of Eq. 2. There are no significant internal correlations between independent variables (Table 5). Figure 4 displays the plot of observed *vs.* calculated log(IC_{50}).

Table 4. Beta coefficients and t-test for significance of coefficients in Eq. 2

Variable	Beta	t(12)	p-level
S_{10}^{N}(LUMO+2)*	-0.72	-7.14	<0.00001
F_{15}(HOMO-1)*	-0.48	-4.84	<0.0004
S_{20}^{N}(LUMO+2)*	-0.29	-2.94	<0.01

Table 5. Matrix of squared correlation coefficients for the variables in Eq. 2

	S_{10}^{N}(LUMO+2)*	F_{15}(HOMO-1)*	S_{20}^{N}(LUMO+2)*
S_{10}^{N}(LUMO+2)*	1.00		
F_{15}(HOMO-1)*	0.04	1.00	
S_{20}^{N}(LUMO+2)*	0.02	0.00	1.00

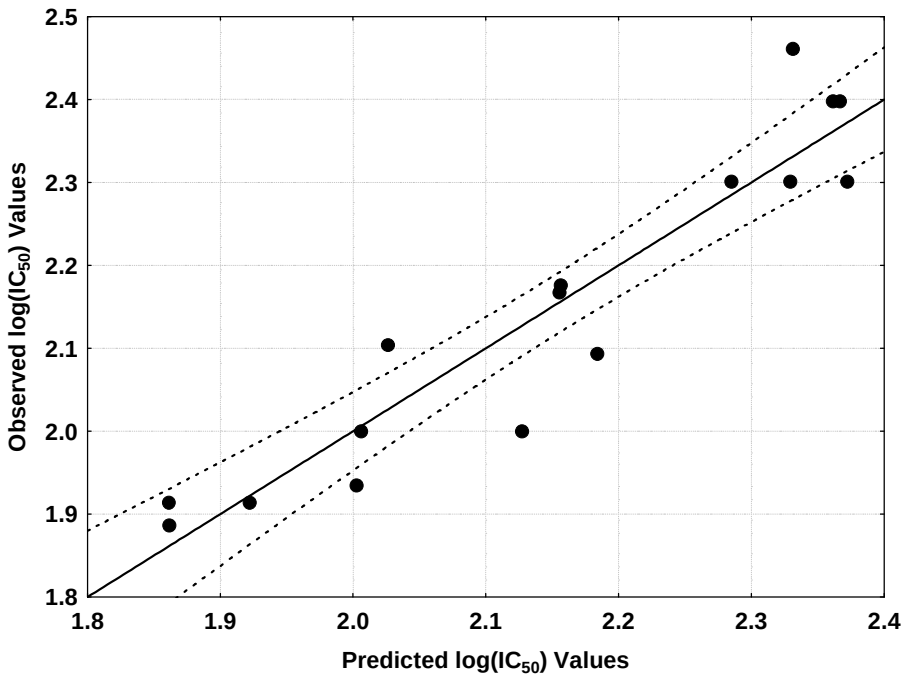

Figure 4. Plot of predicted *vs*. observed log(IC_{50}) values (Eq. 2). Dashed lines denote the 95% confidence interval

The associated statistical parameters of Eq. 2 indicate that this equation is statistically significant and that the variation of the numerical values of a group of three local atomic reactivity indices of atoms of the common skeleton explains only about 86% of the variation of log(IC_{50}) in this group of coumarin derivatives. Figure 4, spanning only about 0.6 orders of magnitude, shows that there is a relatively good correlation of observed *versus* calculated values.

Results for the inhibition of CYP19.
The best equation obtained was:

$$\log(IC_{50})=1.53-0.25S_{16}^{N}(LUMO+1)^{*}-0.07S_{9}^{N}(LUMO+2)^{*}+0.39Q_{2} \quad (3)$$

with n=16, R=0.93, R^2=0.87, adj-R^2=0.84, F(3,12)=26.55 (p<0.00001) and SD=0.10. No outliers were detected and no residuals fall outside the ±2σ limits. Here, S_{16}^N(LUMO+1)* is the nucleophilic superdelocalizability of the second lowest MO localized on atom 16, S_9^N(LUMO+2)* is the nucleophilic superdelocalizability of the third lowest MO localized on atom 9 and Q_2 is the net charge of atom 2. Tables 6 and 7 show the beta coefficients, the results of the t-test for significance of coefficients and the matrix of squared correlation coefficients for the variables of Eq. 3. There are no significant internal correlations between independent variables (Table 7). Figure 5 displays the plot of observed *vs.* calculated log(IC_{50}).

Table 6. Beta coefficients and t-test for significance of coefficients in Eq. 3

	Beta	t(12)	p-level
S_{16}^N(LUMO+1)*	-0.60	-4.97	<0.0003
S_9^N(LUMO+2)*	-0.42	-4.02	<0.002
Q_2	0.34	2.79	<0.02

Table 7. Matrix of squared correlation coefficients for the variables in Eq. 3

	S_{16}^N(LUMO+1)*	S_9^N(LUMO+2)*	Q_2
S_{16}^N(LUMO+1)*	1.00		
S_9^N(LUMO+2)*	0.00	1.00	
Q_2	0.24	0.01	1.00

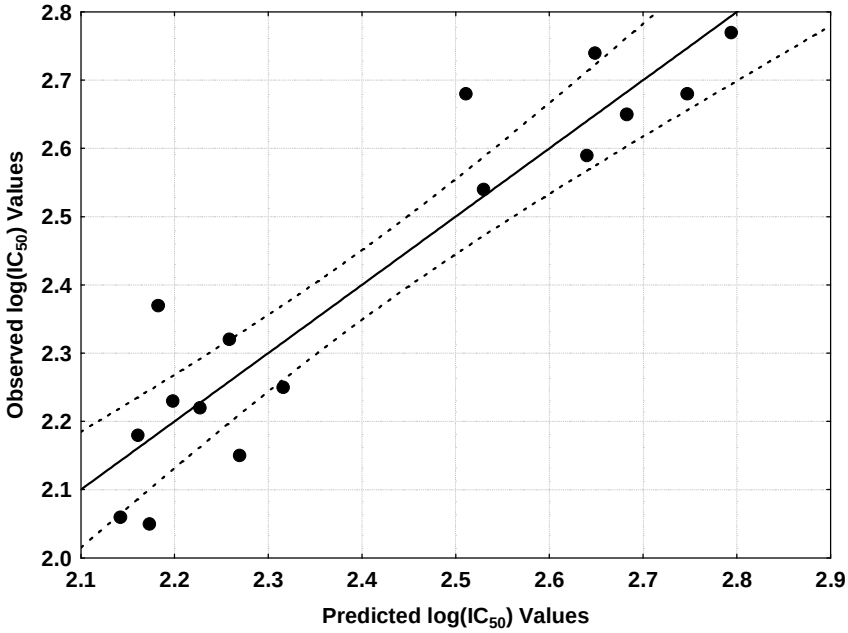

Figure 5. Plot of predicted *vs*. observed log(IC_{50}) values (Eq. 3). Dashed lines denote the 95% confidence interval

The associated statistical parameters of Eq. 3 indicate that this equation is statistically significant and that the variation of the numerical values of a group of three local atomic reactivity indices of atoms of the common skeleton explains only about 84% of the variation of log(IC_{50}) in this group of coumarin derivatives. Figure 5, spanning only about 0.7 orders of magnitude, shows that there is a relatively good correlation of observed *versus* calculated values.

Local Molecular Orbitals.

Tables 8 and 9 show the local MO structure of atoms with reactivity indices appearing in Eq. 1, 2 and 3 (see Fig. 2). Nomenclature: Molecule (HOMO) / (HOMO-2)* (HOMO-1)* (HOMO)* - (LUMO)* (LUMO+1)* (LUMO+2)*. All local MOs of atom 20 of the common skeleton (Fig. 2) have a σ nature.

Table 8. Local molecular orbitals of atoms 1, 9, 10 and 15

Mol.	Atom 1	Atom 9	Atom 10	Atom 15
1(87)	78σ83π85π-89π90π91π	85π86π87π-88π89π90π	85π86π87π-88π89π90π	81σ86π87π-88π89π92σ
2 (91)	82σ88π89π-93π94π95π	88π90π91π-92π93π94π	88π90σ91π-92π93π94π	85σ90π91π-92π93π96π
3 (91)	81σ88π89π-93π95π96π	88π90π91π-92π94π95π	89π90π91π-92π93π94π	85σ90π91π-92π94π96π
4 (95)	86σ92π93π-97π98π99π	92π94π95π-96π97π99π	93π94π95π-96π97π99π	89σ94π95π-96π99π100π
5 (103)	94σ97π99π-105π106π114σ	99π101π102π-104π106π107π	95π101π102π-104π106π107π	98σ100σ102π-104π107π108π
6 (107)	96π104π105π-109π111π112π	104π106π107π-108π109σ110π	105π106π107π-108π109π110π	101σ106π107π-108π109π110π
7 (98)	89π91π92π-99π101π103π	96π97π98π-100π102π103π	96π97π98π-100π102π103π	94σ97π98π-100π102π103π
8 (95)	93π94π95π-97π99π100π	92π93π95π-96π97π98π	92π93π95π-96π98π100π	89σ93π95π-96π98π99π
9 (95)	89π92π93π-97π98π99π	92π94π95π-96π97π99π	93π94π95π-96π97π99π	90σ94π95π-96π99π100π
10 (107)	101π104π105π-109π110π111π	105π106π107π-108π110π111π	105π106π107π-108π110π111π	102σ106π107π-108π111π112π
11 (98)	90σ91π92π-99π101π103π	96π97π98π-100π102π103π	96π97π98π-100π102π103π	94σ97π98π-100π102π103π
12 (95)	86π91π94π-97π98π99π	92π93π95π-96π97π99π	92π93π95π-96π97π98π	89σ93π95π-96π97π98π
13 (103)	94π99π102π-105π106π107π	100π101π103π-104π105π107π	100π101π103π-104π105π106π	96σ97σ103π-104π105π106π
14 (103)	94π99π102π-105π106π107π	100π101π103π-104π105π107π	100π101π103π-104π105π106π	96σ97σ103π-104π105π106π
15 (95)	90π92π93π-97π98π99π	92π94π95π-96π97π98π	93π94π95π-96π97π98π	89σ94π95π-96π97π98π
16 (95)	90π92π93π-97π98π99π	93π94π95π-96π98π99π	93π94π95π-96π98π99π	90σ94π95π-96π98π100π
17 (103)	100π102π103π-106π107π111σ	101π102π103π-104π105π106π	101π102π103π-104π105π108π	101π102π103π-104π105π108π
18 (111)	105σ109π111π-114π115π116π	107π108π110π-112π113π114π	107π108π110π-112π113π114π	104σ108π110π-112π113π115π

Table 9. Local molecular orbitals of atoms 16, 18 and 22

Mol.	Atom 16	Atom 18	Atom 22
1(87)	81σ86π87π-88π89π90π	85π86π87π-88π89π90π	82σ86π87π-93π94σ98σ
2 (91)	85σ90π91π-92π93π94π	89π90π91π-92π93π94π	86σ90π91π-97π98π101σ
3 (91)	85σ90π91π-92π94π96π	88π89π90π-92π94π96π	87σ90π91π-97π98π101σ
4 (95)	89σ94π95π-96π99π100π	92π93π94π-96π99π100π	91σ94π95π-101π103π106σ
5 (103)	98σ100σ102π-104π107π108π	98σ101π102π-104π107π108π	98σ100σ103π-109π110σ111σ
6 (107)	101σ106π107π-108π110π112π	104π105π106π-108π110π112π	103σ106π107π-113π114π117σ
7 (98)	94σ97π98π-100π102π109π	94σ96π97π-100π102π104π	95σ97π98π-105π106π109σ
8 (95)	89σ93π95π-96π98π100π	92π93π95π-96π98π100π	93π94π95π-101π102π105σ
9 (95)	90σ94π95π-96π99π100π	92π93π94π-96π99π100π	91σ94π95π-101π103π106σ
10 (107)	102σ106π107π-108π111π112π	104π105π106π-108π111π112π	103σ106π107π-113π114π117σ
11 (98)	94σ97π98π-100π102π108	94σ96π97π-100π102π104π	95σ97π98π-105π106σ107σ
12 (95)	89σ93π95π-96π97π98π	92π93π95π-96π97π98π	90σ93π95π-101π102π105σ
13 (103)	97σ101π103π-104π105π108π	100π101π103π-104π105π106π	98σ101π103π-109π110π114σ
14 (103)	97σ101π103π-104π105π108π	100π101π103π-104π105π108π	98σ101π103π-109π110π114σ
15 (95)	89σ94π95π-96π98π100π	92π93π94π-96π97π98π	91σ94π95π-101π102π105σ
16 (95)	90σ94π95π-96π98π99π	92π93π94π-96π98π99π	91σ94π95π-101π103π106σ
17 (103)	101π102π103π-104π105π108π	99π100π101π-104π105π108π	101π102π103π-109π110π113σ
18 (111)	104σ108π110π-112π113π115π	107π108π110π-112π113π115π	106σ108π110π-117π118π122σ

DISCUSSION

A point that needs to be emphasized is that LMRA equations include only those variables for which the simultaneous variation of their numerical values gives an account of the variation of the value of the biological

property in the group of molecules under analysis. Therefore, the indices participating in the inhibitory process but having constant numerical values will not appear in the final equations. Eq. 1 shows that there is a direct relationship between the variation of the numerical value of a group of local atomic reactivity indices and the variation of the inhibitory potency against CYP11B1. The same happens for Eqs. 2 and 3. In the following we shall discuss the results for each case.

Discussion of the results for the inhibition of CYP11B1.

The beta values (Table 2) show that the importance of variables in Eq. 1 is φ_{R3}>> F_{22}(LUMO+2)*> S_{18}^{E}(HOMO)*> F_1(HOMO-2)*. Let us remember that the Fukui indices are always positive and that the electrophilic superdelocaliz abilities are always negative. Considering the sign of the reactivity indices and the associated sign in Eq. 1, we can see that a high inhibitory activity is associated with a high value of the R_3 orientational parameter, a high value of the electron population of $(HOMO-2)_1^*$, a small value of the electron population of $(LUMO+2)_{22}^*$ and with a high value of S_{18}^{E}(HOMO)*. We shall analyze the variable one by one without forgetting that it is the *simultaneous* variation of their numerical values that gives an account of the variation of the activity in this series. The R_3 substituents have very different effects on the aromatic ring A (Table 1). A large value for φ_{R3} means that we must select substituent with larger values for this index but having similar electronic effects on ring A. We suggest employing substituents such as $(CH_2)_n$Me or $(CH_2)_n$OMe (with n≥1). Atom 1 is a carbon in ring A (Fig 2). The appearance of $(HOMO-2)_1^*$ indicates that $(HOMO-1)_1^*$ and $(HOMO)_1^*$ also participate in the interaction with the site. Table 8 shows that $(HOMO-1)_1^*$ and $(HOMO)_1^*$ have a π nature, while $(HOMO-2)_1^*$ has σ nature in some molecules and π nature in others. The only way to explain this findings is by suggesting that atom 1 is interacting with a π electron deficient center through the π MOs and with another site with empty σ MOs via a C-H..C (or analogous) interaction. Atom 22 is a carbon in ring D (Fig. 2). $(LUMO+2)_{22}^*$ has a σ nature, $(LUMO)_{22}^*$ has a π nature while $(LUMO+1)_{22}^*$ has π or σ natures (Table 9). The plot of the inhibitory activity *versus* F_{22}(LUMO)* and F_{22}(LUMO+1) (not shown) does not provide extra information. Therefore we suggest that atom 22 interacts with occupied π MOs and that an optimal situation is when $(LUMO+2)_{22}^*$ σ population is minimal or does not exist. Atom 18 is oxygen in ring C (Fig. 2). A high inhibitory activity is associated with a high value of S_{18}^{E}(HOMO)*. Table 9 shows that the local HOMO* has a π nature in all molecules. Therefore, atom 18 is interacting with an electron-deficient center through π-π stacked, π-π T-shaped and/or π-cation interactions. All the suggestions are displayed in the partial 2D pharmacophore of Fig. 6.

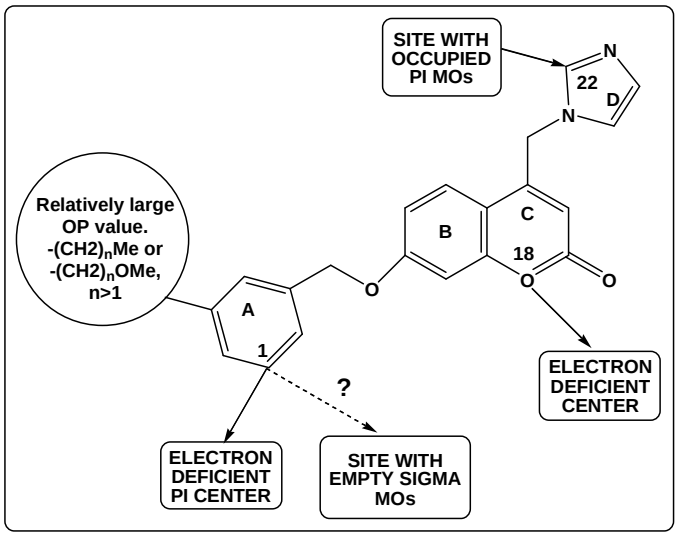

Figure 6. Partial 2D pharmacophore for the inhibition of CYP11B1

Discussion of the results for the inhibition of CYP11B2.

The beta values (Table 4) show that the importance of variables in Eq. 2 is S_{10}^{N}(LUMO+2)*>> F_{15}(HOMO-1)* >> S_{20}^{N}(LUMO+2)*. Considering the sign of the reactivity indices and the associated sign in Eq. 2, we can see that a high inhibitory activity is associated with a high numerical value of F_{15}(HOMO-1)*. The numerical values of the nucleophilic superdelocalizabilities can be positive or negative. In earlier papers we have shown that if we carry an

analysis for positive values, the conclusions are also valid for negative values [50]. If the numerical values for S_{10}^N(LUMO+2)* and S_{20}^N(LUMO+2)* are positive, a high inhibitory capacity is associated with large values of these indices. Atom 15 is a carbon in ring C (Fig. 2). Table 8 shows that $(HOMO-1)_{15}^*$ has a π nature in almost all the molecules. In three molecules this OM has a σ nature. $(HOMO)_{15}^*$ has a π nature in all molecules (Table 8). A large value for F_{15}(HOMO-1)* is associated with a high inhibitory activity. Therefore, we suggest that atom 15 is interacting with a π electron deficient center. The participation of $(HOMO-1)_{15}^*$ with a σ character can be explained in two ways. The first one is that these MOs do not interact with the π electron deficient center. The other one is that these MOs interact with vacant σ MOs. Both suggestions are not incompatible. Atom 10 is a carbon in ring B (Fig. 2). If the numerical values of S_{10}^N(LUMO+2)* are positive, a high inhibitory activity is associated with large numerical values for this reactivity index. Table 10 shows that the three lowest vacant local MOs of atom 10 are of π nature. Larger numerical values for this index are obtained mainly by lowering the energy of the associated MO, making it more reactive. Therefore, we suggest that atom 10 is interacting with a π electron-rich center through at least its three lowest vacant MOs. As we said before, the same conclusions are reached if the numerical values of S_{10}^N(LUMO+2)* negative. Atom 20 is a carbon linking rings C and D (Fig. 2). All the local MOs of this atom have a σ nature. With a similar reasoning employed for atom 10 but also considering the nature of the MOs, we suggest that atom 20 is interacting with a site having occupied MOs of σ nature. Being alkyl chains the most probable sites for this interaction we also suggest the possible existence of a hydrophobic pocket. All the suggestions are displayed in the partial 2D pharmacophore of Fig. 7.

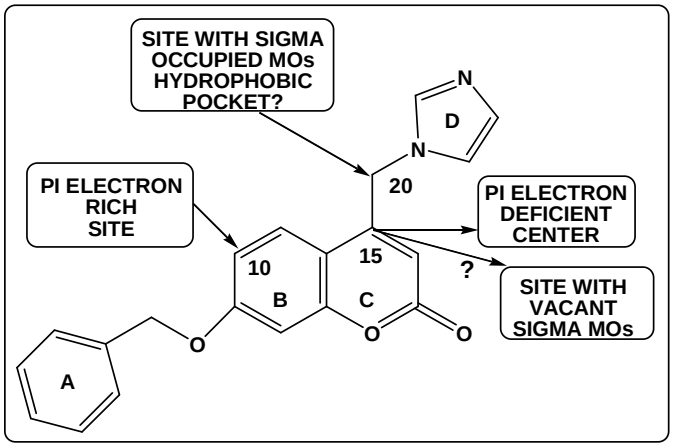

Figure 7. Partial 2D pharmacophore for the inhibition of CYP11B2

Discussion of the results for the inhibition of CYP19.

The beta values (Table 6) show that the importance of variables in Eq. 3 is S_{16}^N(LUMO+1)*> S_9^N(LUMO+2)*> Q_2. Considering the sign of the reactivity indices and the associated sign in Eq. 3, we can see that a high inhibitory activity is associated with negative values for Q_2. In the case that the numerical values of the nucleophilic superdelocalizabilities are positive, a high inhibitory activity is associated with large positive numerical values for these reactivity indices. Atom 2 is a carbon in ring A (Fig. 2). As a negative net charge is associated with a higher inhibitory activity, R_4 substituents (Fig. 1) directly donating electrons to atom 2 are suggested. The only restriction is that their OP values be within the numerical limits of the ones appearing in Table 1. Atom 2 could be interacting with a positively-charged center. Atom 16 is a carbon in ring C (Fig. 2). Table 9 shows that $(LUMO)_{16}^*$ and $(LUMO+1)_{16}^*$ have a π nature. Employing the same reasoning used above for similar cases, we suggest that atom 16 is interacting with an electron-rich center thorough its first two lowest vacant MOs. Atom 9 is a carbon in ring B (Fig. 2). Table 9 shows that the three lowest vacant MOs have a π nature. Employing the same reasoning used above for similar cases, we suggest that atom 16 is interacting with an electron-rich center thorough its first three lowest vacant MOs. All the suggestions are displayed in the partial 2D pharmacophore of Fig. 8.

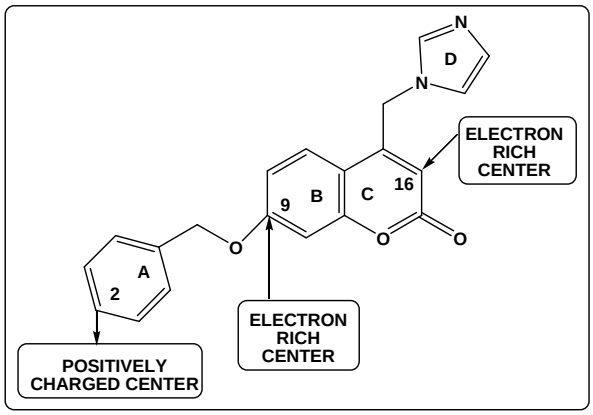

Figure 8. Partial 2D pharmacophore for the inhibition of CYP19

Life on Earth originated 3.5-3.8 billion years ago as a complex sequence of chemical reactions. Along all this time, the environmental conditions and the change in the heritable characteristics of biological populations over successive generations produced more and more complex living structures. *Homo sapiens*, the only extant member of the genus *Homo*, is the one of the actual products. Inside us, extremely complex molecular interactions occur at many levels of organization. All them have a fundamental characteristic: they must be highly specific in order to conserve the stability of the many subsystems. At the cellular level, the communications between cells are carried out by proteins, amino acids, steroids and several other substances (the signaling molecules), while large proteins are the receptors of the messages. Other proteins in the cell membrane, linked with the receptors, transfer the message to the interior of the cell. To prevent any disruption of the living systems, a high degree of complementarity between the messengers and their receptors exists. This is called the key and lock principle. When a messenger molecule travels in the interior milieu it needs to be recognized by its receptor and then guided to reach the final interaction geometry. At larger distances this process is controlled by the molecular electrostatic potential structure. At intermediate distances, a mixture of electrostatic and weak MO-MO interactions probably guides and orientates the messenger molecule. At the end of the process, short-range interactions such as hydrogen bonds help to finalize the binding process. Generally speaking, the specificity of the lock is due to the three dimensional (3D) arrangement of charged sites and occupied and virtual molecular orbitals. Only those molecules fitting perfectly this 3-D network will be able to produce a biological effect, while others than can partially bind the lock only will block it. These electrostatic and MO-MO interactions are included in the Klopman expression that is an important part of the foundations of the KPG method [62]. This specificity is reflected in this paper in the fact that all three inhibitory processes are orbital-controlled. We have perceived this fact along all the history of the applications of the KPG method to many different series of molecules interacting with macromolecular structures or exerting definite biological activities. Our ancestors discovered by trial and error that some chemicals existing in some plants, mushrooms and animals can produce altered states of consciousness, cure, paralyze, kill, etc. This is so because these molecules can interact with the lock by mimicking the electronic and conformational characteristics of the endogenous messenger(s).

Rings A, B-C and D are not coplanar in all molecules (see Fig. 9 for example). Fig. 1 and Table 1 show that all substituents are only in ring A but Eq. 1-3 show also reactivity indices belonging to rings B-C and D. This is so because the change of substituents modifies the number, nature and localization of molecular orbitals (more or fewer π, lone pair and/or σ MOs). Perhaps this is the main reason to carry out electronic structure calculations when designing new molecules. Unhappily, there are no known rules to predict these long-range substituent effects.

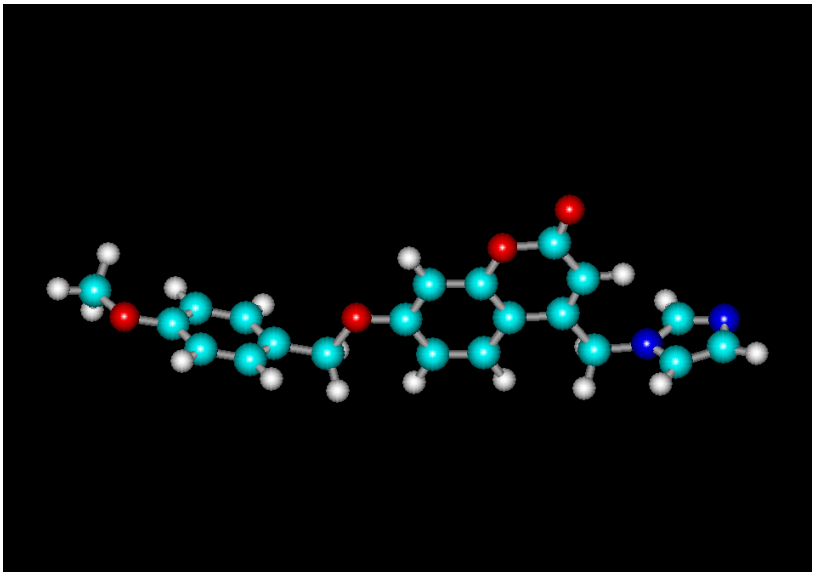

Figure 9. Fully optimized geometry of molecule 12

The calculations were done after full geometry optimization. But there is no way to know if this conformation is the active one. This is the reason of the two dimensional representation of the partial pharmacophores.

Some words about the concept of local molecular orbitals. This concept arises directly from the fact that in large molecules the frontier molecular orbitals (molecular HOMO and LUMO) sometimes are not localized on all the molecule. As an example, Fig. 10 displays the HOMO of molecule 1.

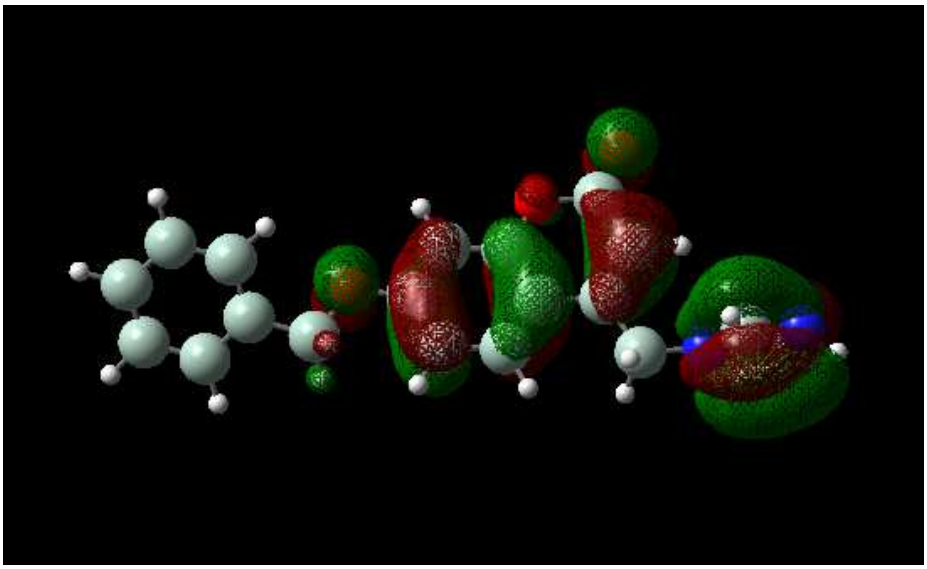

Figure 10. Highest Occupied Molecular Orbital (HOMO) of molecule 1

We can see that this MO is localized on rings B, C and D, but not on ring A. For this case, we say that in the case of most atoms of rings B, C and D, the highest occupied local molecular orbital, HOMO*, coincides with the molecular HOMO. Figure 11 shows the second highest occupied MO of molecule 1.

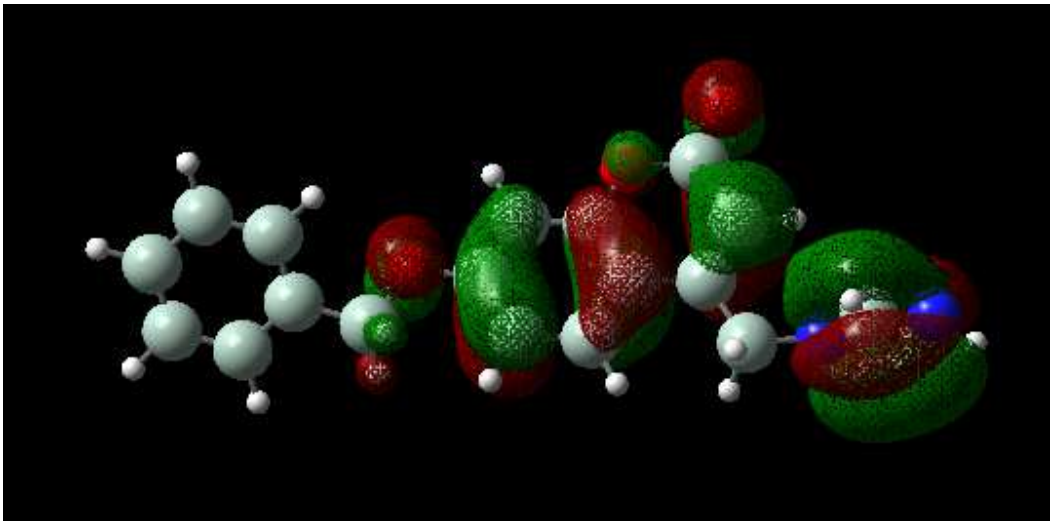

Figure 11. Second Highest Occupied Molecular Orbital (HOMO-1) of molecule 1

Again, this MO is not localized on ring A. In this case we say that in the case of most atoms of rings B, C and D, their second highest occupied local molecular orbital, (HOMO-1)*, coincides with the HOMO-1 of the molecule. Figure 12 shows the third highest occupied MO of molecule 1.

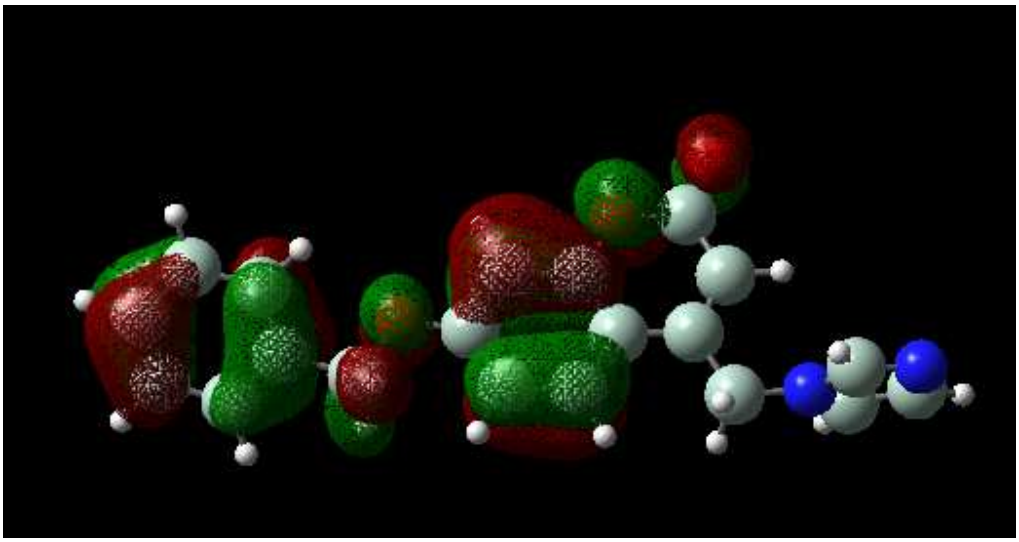

Figure 12. Third Highest Occupied Molecular Orbital (HOMO-2) of molecule 1

(HOMO-2) is localized on rings A and B. Now, we say that for the atoms of ring A their highest occupied local MO, HOMO*, coincides with the molecule's (HOMO-2). For the atoms of ring B we say that their third highest occupied local MO, (HOMO-2)*, coincides with the molecule's (HOMO-2). These facts are summarized in Tables 8 and 9.

In summary, we have obtained statistically significant relationships between the variation of some local atomic reactivity indices and the variation of the inhibitory potencies against steroid 11β-hydroxylase, aldosterone synthase and aromatase in a series of coumarin derivatives. The corresponding partial pharmacophores were built and some suggestions to improve the inhibitory potency have been presented.

REFERENCES

[1] Stefanachi, N. Hanke, L. Pisani, F. Leonetti, O. Nicolotti, M. Catto, S. Cellamare, R. W. Hartmann, A. Carotti, *European Journal of Medicinal Chemistry*, **2015,** 89, 106-114.
[2] D. F. V. Lewis, *Cytochromes P450: structure, function and mechanism*, Taylor & Francis, London, **1996**.
[3] P. R. Ortiz de Montellano, *Cytochrome P450: structure, mechanism, and biochemistry*, Springer, Heidelberg, **2015**.
[4] D. Schomburg, G. Michal, *Biochemical Pathways: An Atlas of Biochemistry and Molecular Biology*, John Wiley & Sons, Hoboken, N.J., **2012**.
[5] M. I. New, O. Lekarev, A. Parsa, T. T. Yuen, B. O'Malley, G. D. Hammer, *Genetic steroid disorders*, Academic Press, **2013**.
[6] K. Yi, L. Yang, Z. Lan, M. Xi, *Eur. J. Obst. Gynecol. Rep. Biol.*, **2016,** 199, 42-48.
[7] H.-H. Nguyen, A. Eiden-Plach, F. Hannemann, E. M. Malunowicz, M. F. Hartmann, S. A. Wudy, R. Bernhardt, *J. Steroid Biochem. Mol. Biol.*, **2016,** 155, Part A, 126-134.
[8] A. Bogacz, J. Bartkowiak-Wieczorek, D. Procyk, A. Seremak-Mrozikiewicz, M. Majchrzycki, K. Dziekan, A. Bienert, B. Czerny, *Eur. J. Obst. Gynecol. Rep. Biol.*, **2016,** 197, 11-15.
[9] L. Xu, W. Xia, X. Wu, X. Wang, L. Zhao, M. Nie, *Steroids*, **2015,** 101, 51-55.
[10] X. Wang, E. R. Simpson, K. A. Brown, *J. Steroid Biochem. Mol. Biol.*, **2015,** 153, 35-44.
[11] X. Wang, M. Nie, L. Lu, A. Tong, S. Chen, Z. Lu, *Steroids*, **2015,** 100, 11-16.
[12] T. P. M. Nguyen, T. H. Nguyen, D. N. Ngo, C. D. Vu, T. K. L. Nguyen, V. H. Nong, H. H. Nguyen, *Gene*, **2015,** 565, 291-294.
[13] A. H. Straume, S. Knappskog, P. E. Lønning, *J. Steroid Biochem. Mol. Biol.*, **2012,** 128, 69-75.
[14] B. Rumianowski, G. Adler, K. Safranow, A. Brodowska, B. Karakiewicz, S. Słuczanowska-Głąbowska, B. Łoniewska, M. Piasecka, A. Ciechanowicz, M. Laszczyńska, *Reprod. Biol.*, **2012,** 12, 368-373.
[15] W. Lv, J. Liu, T. C. Skaar, E. O'Neill, G. Yu, D. A. Flockhart, M. Cushman, *J. Med. Chem.*, **2016,** 59, 157-170.
[16] J. P. N. Papillon, C. Lou, A. K. Singh, C. M. Adams, G. M. Ksander, M. E. Beil, W. Chen, J. Leung-Chu, F. Fu, L. Gan, C.-W. Hu, A. Y. Jeng, D. LaSala, G. Liang, D. F. Rigel, K. S. Russell, J. A. Vest, C. Watson, *J. Med. Chem.*, **2015,** 58, 9382-9394.
[17] J. P. N. Papillon, C. M. Adams, Q.-Y. Hu, C. Lou, A. K. Singh, C. Zhang, J. Carvalho, S. Rajan, A. Amaral, M. E. Beil, F. Fu, E. Gangl, C.-W. Hu, A. Y. Jeng, D. LaSala, G. Liang, M. Logman, W. M. Maniara, D. F. Rigel, S. A. Smith, G. M. Ksander, *J. Med. Chem.*, **2015,** 58, 4749-4770.
[18] R. E. Martin, J. D. Aebi, B. Hornsperger, H.-J. Krebs, B. Kuhn, A. Kuglstatter, A. M. Alker, H. P. Märki, S. Müller, D. Burger, G. Ottaviani, W. Riboulet, P. Verry, X. Tan, K. Amrein, A. V. Mayweg, *J. Med. Chem.*, **2015,** 58, 8054-8065.
[19] W. Lv, J. Liu, T. C. Skaar, D. A. Flockhart, M. Cushman, *J. Med. Chem.*, **2015,** 58, 2623-2648.
[20] S. B. Hoyt, W. Petrilli, C. London, G.-B. Liang, J. Tata, Q. Hu, L. Yin, C. J. van Koppen, R. W. Hartmann, M. Struthers, T. Wisniewski, N. Ren, C. Bopp, A. Sok, T.-Q. Cai, S. Stribling, L.-Y. Pai, X. Ma, J. Metzger, A. Verras, D. McMasters, Q. Chen, E. Tung, W. Tang, G. Salituro, N. Buist, J. Clemas, G. Zhou, J. Gibson, C. A. Maxwell, M. Lassman, T. McLaughlin, J. Castro-Perez, D. Szeto, G. Forrest, R. Hajdu, M. Rosenbach, Y. Xiong, *ACS Med. Chem. Lett.*, **2015,** 6, 861-865.
[21] S. B. Hoyt, M. K. Park, C. London, Y. Xiong, J. Tata, D. J. Bennett, A. Cooke, J. Cai, E. Carswell, J. Robinson, J. MacLean, L. Brown, S. Belshaw, T. R. Clarkson, K. Liu, G.-B. Liang, M. Struthers, D. Cully, T. Wisniewski, N. Ren, C. Bopp, A. Sok, T.-Q. Cai, S. Stribling, L.-Y. Pai, X. Ma, J. Metzger, A. Verras, D. McMasters, Q. Chen, E. Tung, W. Tang, G. Salituro, N. Buist, J. Kuethe, N. Rivera, J. Clemas, G. Zhou, J. Gibson, C. A. Maxwell, M. Lassman, T. McLaughlin, J. Castro-Perez, D. Szeto, G. Forrest, R. Hajdu, M. Rosenbach, A. Ali, *ACS Med. Chem. Lett.*, **2015,** 6, 573-578.
[22] C. L. Varela, C. Amaral, G. Correia-da-Silva, R. A. Carvalho, N. A. Teixeira, S. C. Costa, F. M. F. Roleira, E. J. Tavares-da-Silva, *Steroids*, **2013,** 78, 662-669.
[23] M. A. E. Pinto-Bazurco Mendieta, Q. Hu, M. Engel, R. W. Hartmann, *J. Med. Chem.*, **2013,** 56, 6101-6107.
[24] J. Park, L. Czapla, R. E. Amaro, *J. Chem. Inf. Mod.*, **2013,** 53, 2047-2056.
[25] E. L. Meredith, G. Ksander, L. G. Monovich, J. P. N. Papillon, Q. Liu, K. Miranda, P. Morris, C. Rao, R. Burgis, M. Capparelli, Q.-Y. Hu, A. Singh, D. F. Rigel, A. Y. Jeng, M. Beil, F. Fu, C.-W. Hu, D. LaSala, *ACS Med. Chem. Lett.*, **2013,** 4, 1203-1207.
[26] M. G. Ferlin, D. Carta, R. Bortolozzi, R. Ghodsi, A. Chimento, V. Pezzi, S. Moro, N. Hanke, R. W. Hartmann, G. Basso, G. Viola, *J. Med. Chem.*, **2013,** 56, 7536-7551.
[27] L. Yin, S. Lucas, F. Maurer, U. Kazmaier, Q. Hu, R. W. Hartmann, *J. Med. Chem.*, **2012,** 55, 6629-6633.

[28] F. Stauffer, P. Furet, A. Floersheimer, M. Lang, *Bioorg. Med. Chem. Lett.*, **2012,** 22, 1860-1863.
[29] Q. Hu, L. Yin, R. W. Hartmann, *J. Med. Chem.*, **2012,** 55, 7080-7089.
[30] D. Ghosh, J. Lo, D. Morton, D. Valette, J. Xi, J. Griswold, S. Hubbell, C. Egbuta, W. Jiang, J. An, H. M. L. Davies, *J. Med. Chem.*, **2012,** 55, 8464-8476.
[31] L. W. L. Woo, C. Bubert, A. Purohit, B. V. L. Potter, *ACS Med. Chem. Lett.*, **2011,** 2, 243-247.
[32] A. Stefanachi, A. D. Favia, O. Nicolotti, F. Leonetti, L. Pisani, M. Catto, C. Zimmer, R. W. Hartmann, A. Carotti, *J. Med. Chem.*, **2011,** 54, 1613-1625.
[33] F. Caporuscio, G. Rastelli, C. Imbriano, A. Del Rio, *J. Med. Chem.*, **2011,** 54, 4006-4017.
[34] L. Roumen, J. W. Peeters, J. M. A. Emmen, I. P. E. Beugels, E. M. G. Custers, M. de Gooyer, R. Plate, K. Pieterse, P. A. J. Hilbers, J. F. M. Smits, J. A. J. Vekemans, D. Leysen, H. C. J. Ottenheijm, H. M. Janssen, J. J. R. Hermans, *J. Med. Chem.*, **2010,** 53, 1712-1725.
[35] N. W. Jacobsen, B. Halling-Sørensen, F. K. Birkved, *Toxicology in Vitro*, **2008,** 22, 146-153.
[36] M. Häggström, D. Richfield, "Diagram of the pathways of human steroidogenesis," *Wikiversity Journal of Medicine*, vol. 1, no. 1, https://commons.wikimedia.org/wiki/File:Steroidogenesis.svg#file, **2014**.
[37] J. S. Gómez Jeria, *Boll. Chim. Farmac.*, **1982,** 121, 619-625.
[38] J. S. Gómez-Jeria, *Int. J. Quant. Chem.*, **1983,** 23, 1969-1972.
[39] J. S. Gómez-Jeria, *Il Far. (Ed. Sci).* **1985,** 40, 299-302.
[40] J. S. Gómez-Jeria, "Modeling the Drug-Receptor Interaction in Quantum Pharmacology," in *Molecules in Physics, Chemistry, and Biology*, J. Maruani Ed., vol. 4, pp. 215-231, Springer Netherlands, **1989**.
[41] J. S. Gómez-Jeria, M. Ojeda-Vergara, *J. Chil. Chem. Soc.*, **2003,** 48, 119-124.
[42] J. S. Gómez-Jeria, *Elements of Molecular Electronic Pharmacology (in Spanish)*, Ediciones Sokar, Santiago de Chile, **2013**.
[43] J. S. Gómez-Jeria, *Canad. Chem. Trans.*, **2013,** 1, 25-55.
[44] J. S. Gómez-Jeria, M. Flores-Catalán, *Canad. Chem. Trans.*, **2013,** 1, 215-237.
[45] G. A. Kpotin, G. S. Atohoun, U. A. Kuevi, A. Houngue-Kpota, J.-B. Mensah, J. S. Gómez-Jeria, *J. Chem. Pharmaceut. Res.*, **2016,** 8, 1019-1026.
[46] A. Robles-Navarro, J. S. Gómez-Jeria, *Der Pharma Chem.*, **2016,** 8, 417-440.
[47] J. Muñoz-Pérez, P. Leyton, C. Paipa, J. P. Soto, J. Brunet, J. S. Gómez-Jeria, M. M. Campos-Vallette, *Journal of Molecular Structure*, **2016,** 1122, 198-204.
[48] J. S. Gómez-Jeria, Í. Orellana, *Der Pharma Chem.*, **2016,** 8, 476-487.
[49] J. S. Gómez-Jeria, C. Moreno-Rojas, *Der Pharma Chem.*, **2016,** 8, 475-482.
[50] J. S. Gómez-Jeria, M. Matus-Perez, *Der Pharma Chem.*, **2016,** 8, 1-11.
[51] J. S. Gómez-Jeria, V. Gazzano, *Der Pharma Chem.*, **2016,** 8, 21-27.
[52] J. S. Gómez-Jeria, R. Cornejo-Martínez, *Der Pharma Chem.*, **2016,** 8, 329-337.
[53] J. S. Gómez-Jeria, H. R. Bravo, *Der Pharma Chem.*, **2016,** 8, 25-34.
[54] J. S. Gómez-Jeria, S. Abarca-Martínez, *Der Pharma Chem.*, **2016,** 8, 507-526.
[55] H. R. Bravo, B. E. Weiss-López, J. Valdebenito-Gamboa, J. S. Gómez-Jeria, *Res. J. Pharmac. Biol. Chem. Sci.*, **2016,** 7, 792-798.
[56] M. J. Frisch, G. W. Trucks, H. B. Schlegel, G. E. Scuseria, M. A. Robb, J. R. Cheeseman, J. Montgomery, J.A., T. Vreven, K. N. Kudin, J. C. Burant, J. M. Millam, S. S. Iyengar, J. Tomasi, V. Barone, B. Mennucci, M. Cossi, G. Scalmani, N. Rega, "G03 Rev. E.01," Gaussian, Pittsburgh, PA, USA, **2007**.
[57] J. S. Gómez-Jeria, "D-Cent-QSAR: A program to generate Local Atomic Reactivity Indices from Gaussian 03 log files. v. 1.0," Santiago, Chile, **2014**.
[58] J. S. Gómez-Jeria, *J. Chil. Chem. Soc.*, **2009,** 54, 482-485.
[59] J. S. Gómez-Jeria, *Res. J. Pharmac. Biol. Chem. Sci.*, **2016,** 7, 2258-2260.
[60] J. S. Gómez-Jeria, *Res. J. Pharmac. Biol. Chem. Sci.*, **2016,** 7, 288-294.
[61] Statsoft, "Statistica v. 8.0," 2300 East 14 th St. Tulsa, OK 74104, USA, **1984-2007**.
[62] G. Klopman, *J. Am. Chem. Soc.*, **1968,** 90, 223-234.